Supplementaty Information to

Hidden-driver inference reveals synergistic brain-penetrant therapies for medulloblastoma

Liu, et al.

Supplementary Figures 1-10

Supplementary Tables 1-15

Supplementary Figures

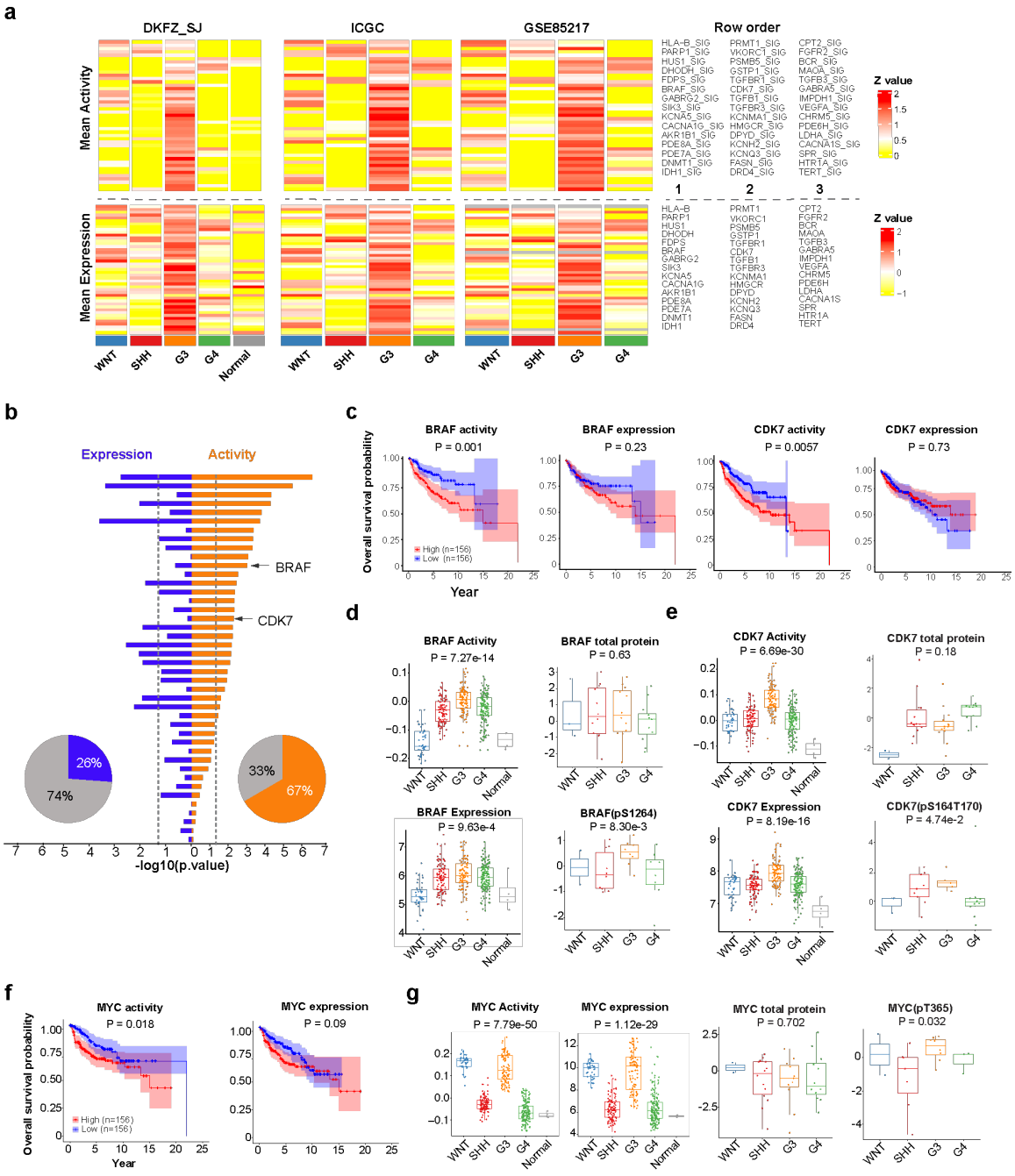

Figure S1. Druggable hidden drivers in high-risk medulloblastoma. a Heatmap displaying druggable hidden driver activities and expressions in three medulloblastoma cohorts. **b** Druggable hidden driver genes identified by the SINBA algorithm were evaluated for association with overall survival in the GSE85217 cohort. MB Patients were stratified by high (>75th percentile) versus low (<25th percentile) gene expression or activity. Kaplan–Meier survival analysis; p values calculated by log-rank test. **c** Kaplan–Meier curves showing overall survival of MB patients stratified by BRAF or CDK7 activity or expression. **d** BRAF activity,

mRNA expression, total protein and phosphorylated BRAF (S1264) levels across MB subgroups and normal samples. **e** CDK7 activity, mRNA expression, total protein and phosphorylated CDK7 (S164/T170) levels across MB subgroups and normal samples. **f** Kaplan–Meier curves showing overall survival of MB patients stratified by MYC activity or expression. **g** MYC activity, mRNA expression, total protein and phosphorylated MYC (T365) levels across MB subgroups and normal samples. For (**d**), (**e**), and (**g**), unpaired two-sided t tests were performed between G3 MB and other subgroups. For (**c**) and (**f**), P value was calculated by log-rank test.

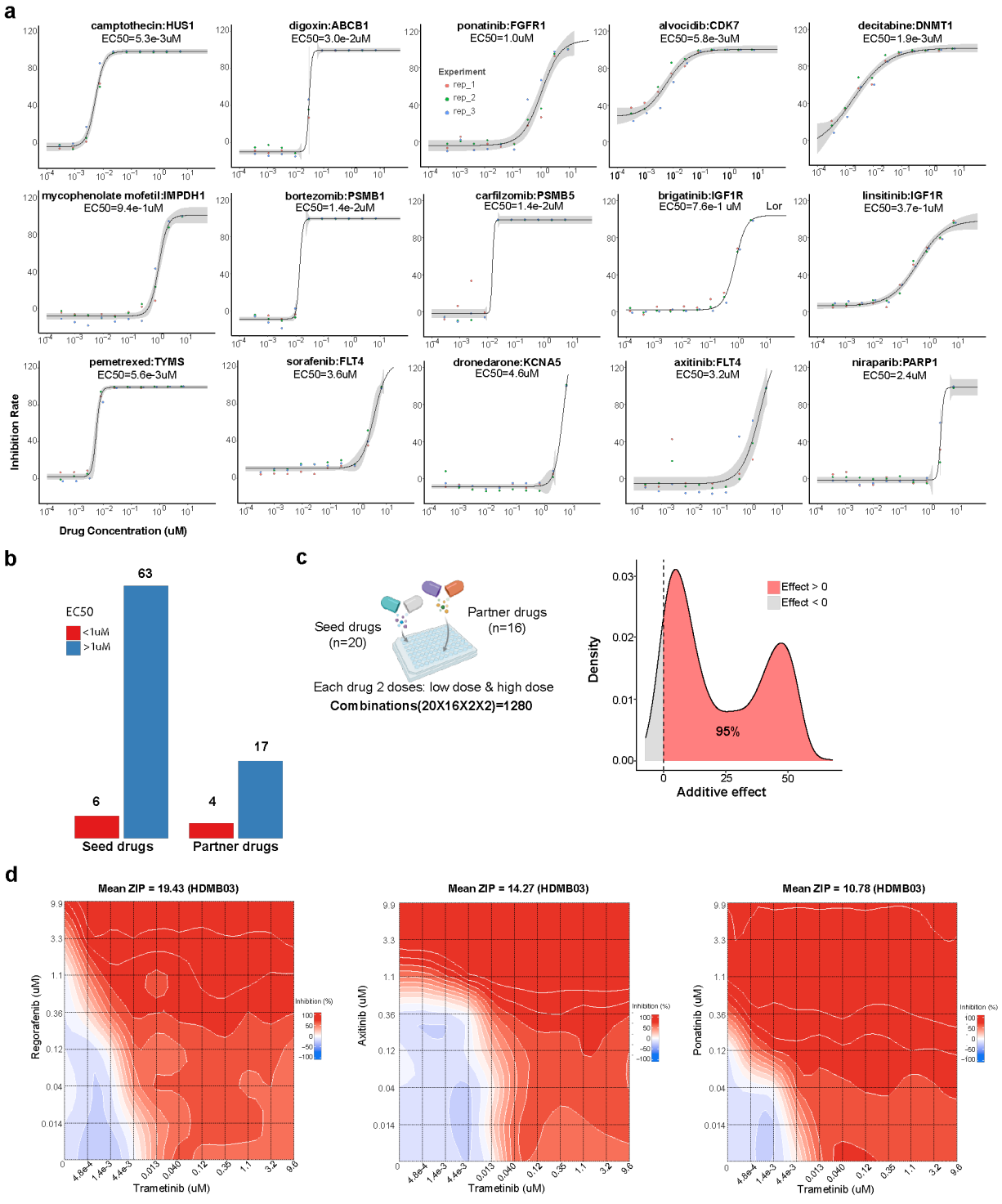

Figure S2. SINBA-guided multi-step drug screening identifies potential therapeutic combinations for high-risk medulloblastoma. a Seed and partner drugs with half-maximal effective concentrations (EC50) below 10 μM.

b Summary of HTS results from the seed drug and partner drug libraries. **c** Overview of two-dose combination screening outcomes. **d** Representative contour plots showing HDMB03 cell growth inhibition across varying concentrations of trametinib, axitinib or ponatinib in combination with regorafenib.

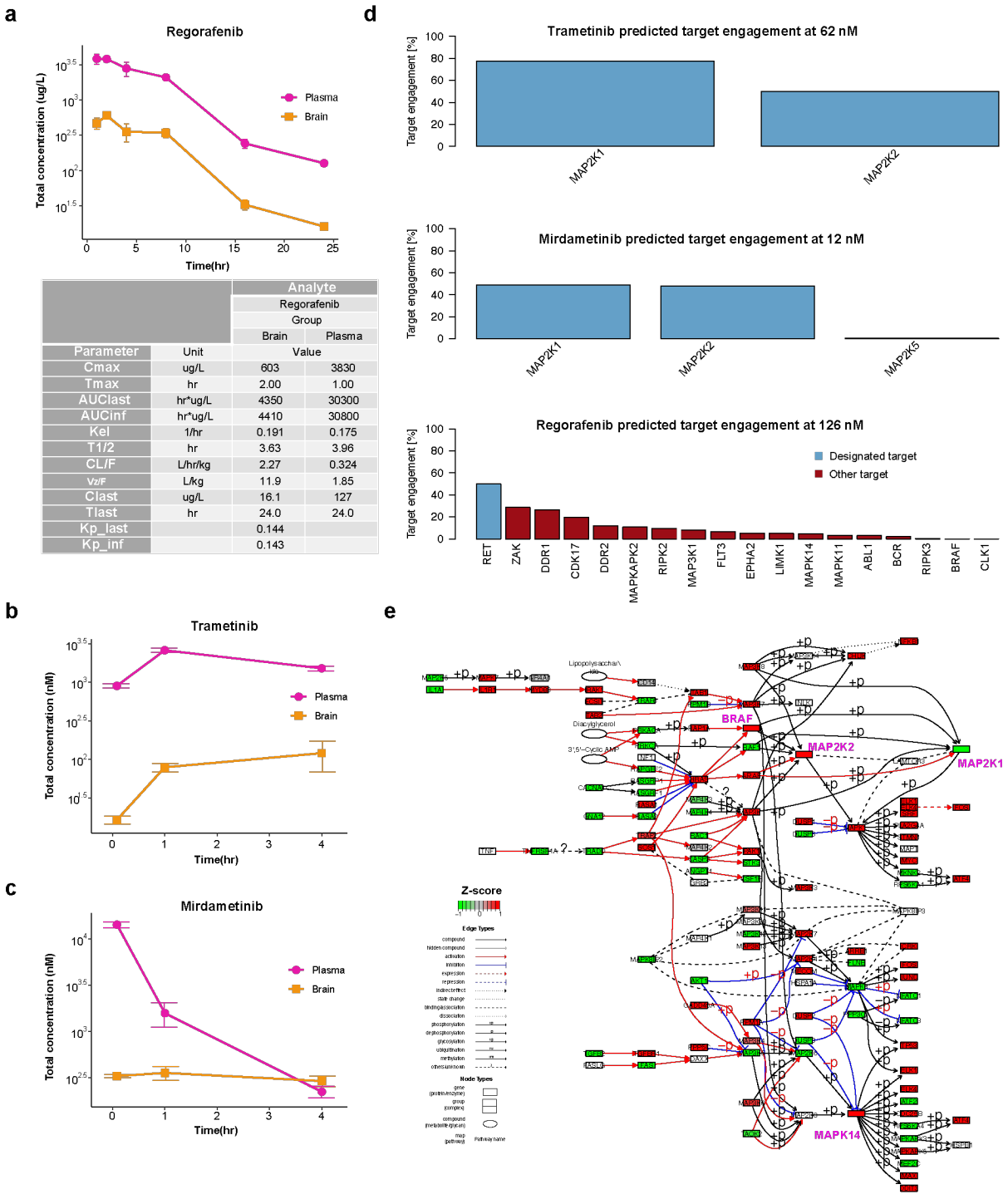

		Analyte	
		Regorafenib	
		Group	
		Brain	Plasma
Parameter	Unit	Value	
Cmax	ug/L	603	3830
Tmax	hr	2.00	1.00
AUClast	hr*ug/L	4350	30300
AUCinf	hr*ug/L	4410	30800
Kel	1/hr	0.191	0.175
T1/2	hr	3.63	3.96
CL/F	L/hr/kg	2.27	0.324
Vz/F	L/kg	11.9	1.85
Clast	ug/L	16.1	127
Tlast	hr	24.0	24.0
Kp_last		0.144	
Kp_inf		0.143	

Figure S3. Pharmacokinetic profile of the MEK inhibitors and regorafenib. a Pharmacokinetic profile of regorafenib: plasma and brain concentrations measured over 24 hours post-dose with the statistical analysis of regorafenib plasma and brain concentration–time (Ct) profiles. **b-c** Pharmacokinetic profiles of

trametinib and mirdametinib: plasma and brain concentrations measured over 4 hours post-dose. **d** Chemical proteomic profiling of clinical kinase inhibitors, showing predicted interaction targets of trametinib, mirdametinib, and regorafenib. **e** Comparative analysis of driver activity within the KEGG MAPK signaling cascade between G3 and normal samples in the DKFZ_SJ cohort. Nodes are color-coded according to Z-score (normalized p value) differentials reflecting G3 versus normal cerebellum. Genes targeted by trametinib and regorafenib are accentuated in magenta. For (**a**), (**b**), and (**c**), each time point data are represented as mean ± SEM.

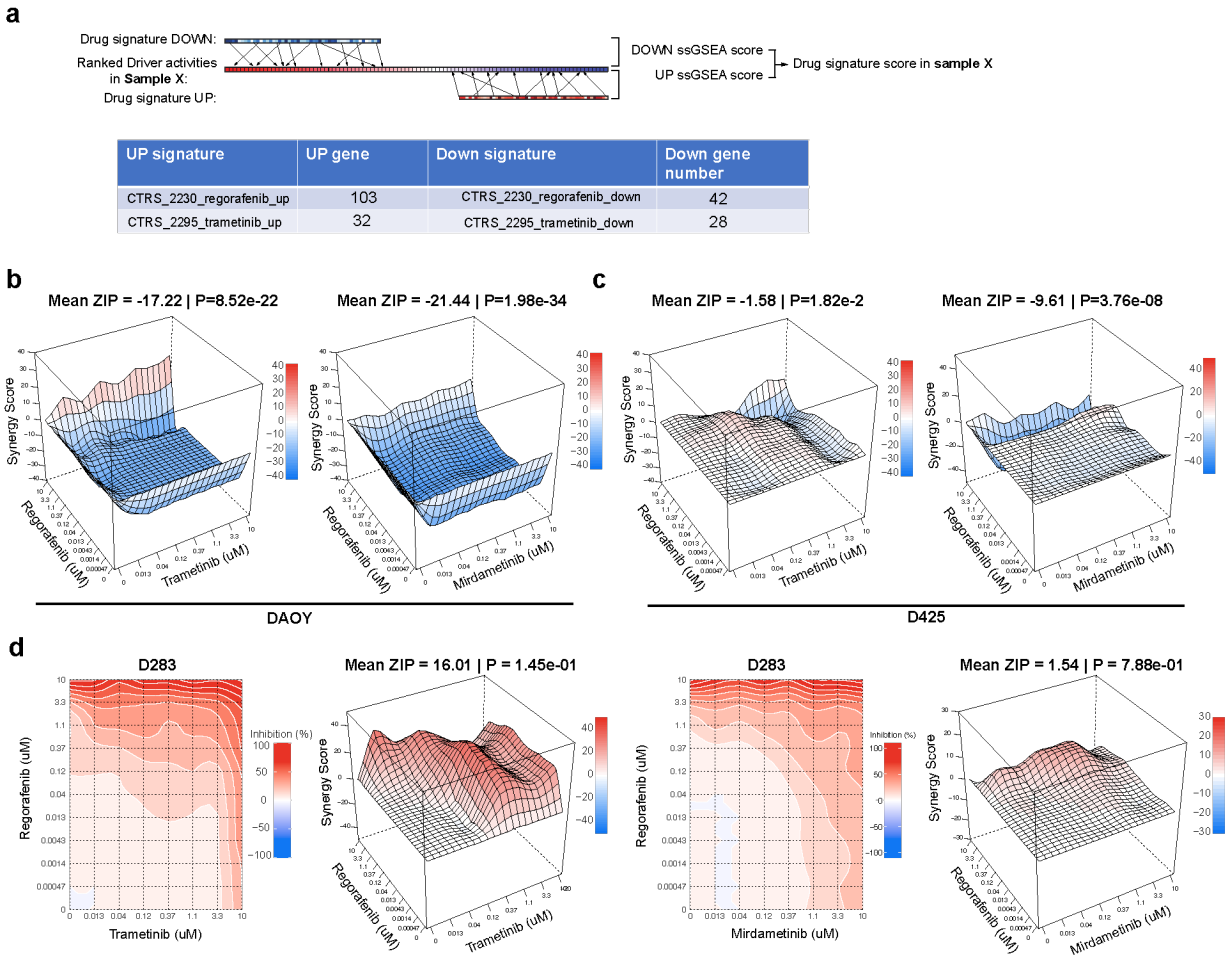

UP signature	UP gene	Down signature	Down gene number
CTRS_2230_regorafenib_up	103	CTRS_2230_regorafenib_down	42
CTRS_2295_trametinib_up	32	CTRS_2295_trametinib_down	28

Figure S4. Drug sensitivity and synergy analysis for MEK inhibitor and regorafenib combinations in medulloblastoma models. a Schematic representation of the drug sensitivity calculation framework, leveraging CNS-specific drug signatures from the iLINCS database to identify responsive medulloblastoma

models. Refer to the Methods section for further details. **b** Surface plots of ZIP synergy score landscapes for trametinib plus regorafenib (left) and mirdametinib plus regorafenib (right) in the DAOY cell line. **c** Surface plots of ZIP synergy score landscapes for trametinib plus regorafenib (left) and mirdametinib plus regorafenib (right) in the D425 cell line. **d** Contour plots of cell viability and surface plots of ZIP synergy score landscapes for trametinib plus regorafenib (left) and mirdametinib plus regorafenib (right) in D283 cells.

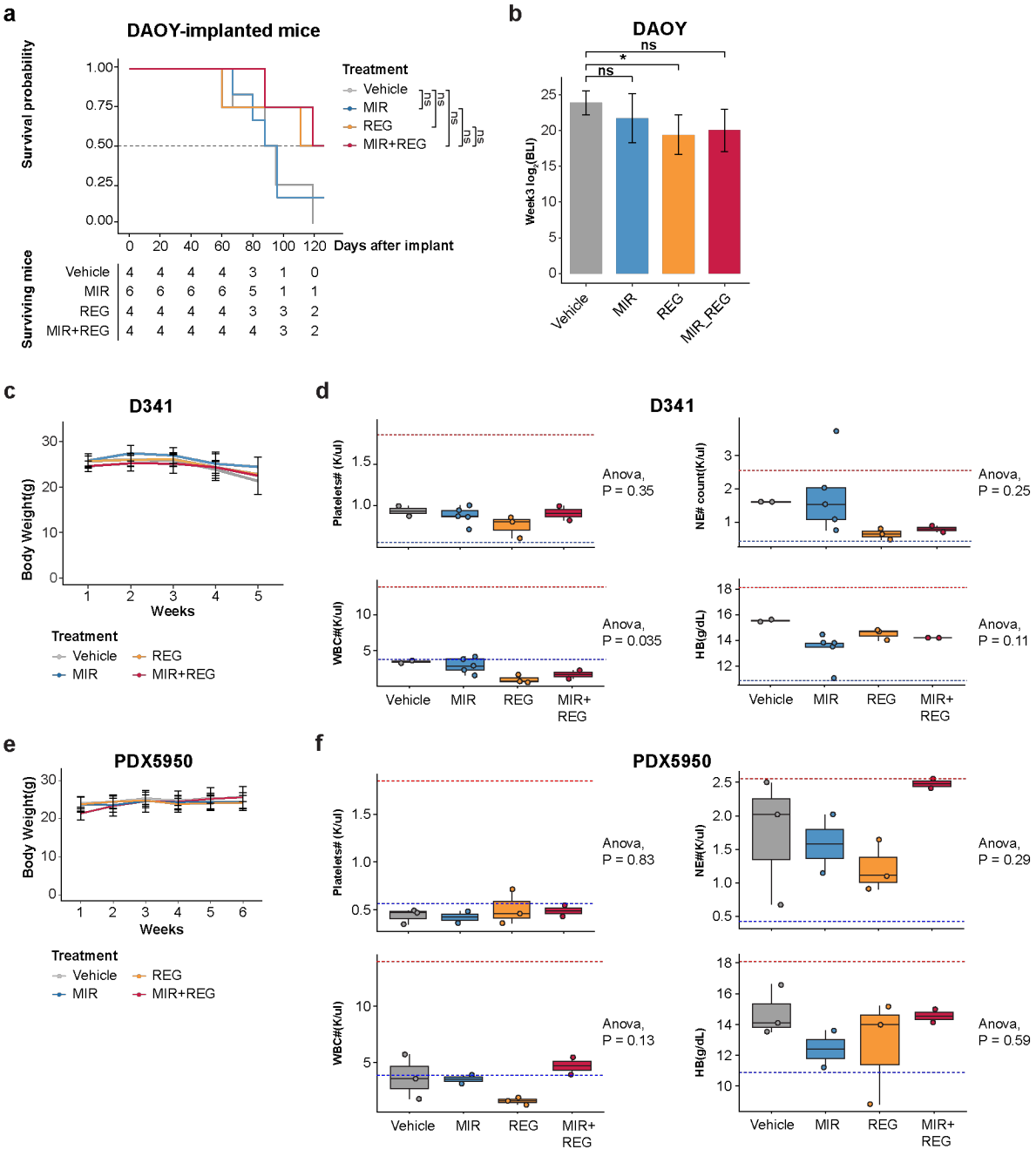

56

57 **Figure S5. The MEKi + regorafenib combination lacks synergistic efficacy in the SHH model DAOY**

58 **and shows no significant toxicity in mice. a** Kaplan–Meier survival curves for mice implanted with DAOY

cells and treated as in Figure 3A. Group sizes (n) are indicated in the risk table; log-rank test: ns, not significant. **b** Quantified bioluminescence imaging (BLI) for each treatment group in the DAOY model at week 3 post-treatment. Data are mean ± SEM. **c** Weekly body weight changes in D341-bearing mice after surgery. Data are represented as mean ± SEM. **d** Endpoint toxicity assessment by complete blood counts (n = 2–4 per group) in the D341 study; dashed lines indicate normal reference ranges. **e** Weekly body weight changes in PDX5950-bearning mice after surgery. Data are represented as mean ± SEM. **f** Endpoint toxicity assessment by complete blood counts (n = 2–4 per group) in the PDX5950 study. For (**b**) unpaired two-sided t tests were used. *P < 0.05, **P < 0.01, ***P < 0.001; ns, not significant.For (**d**) and (**f**), one-way ANOVA was performed among treatment groups.

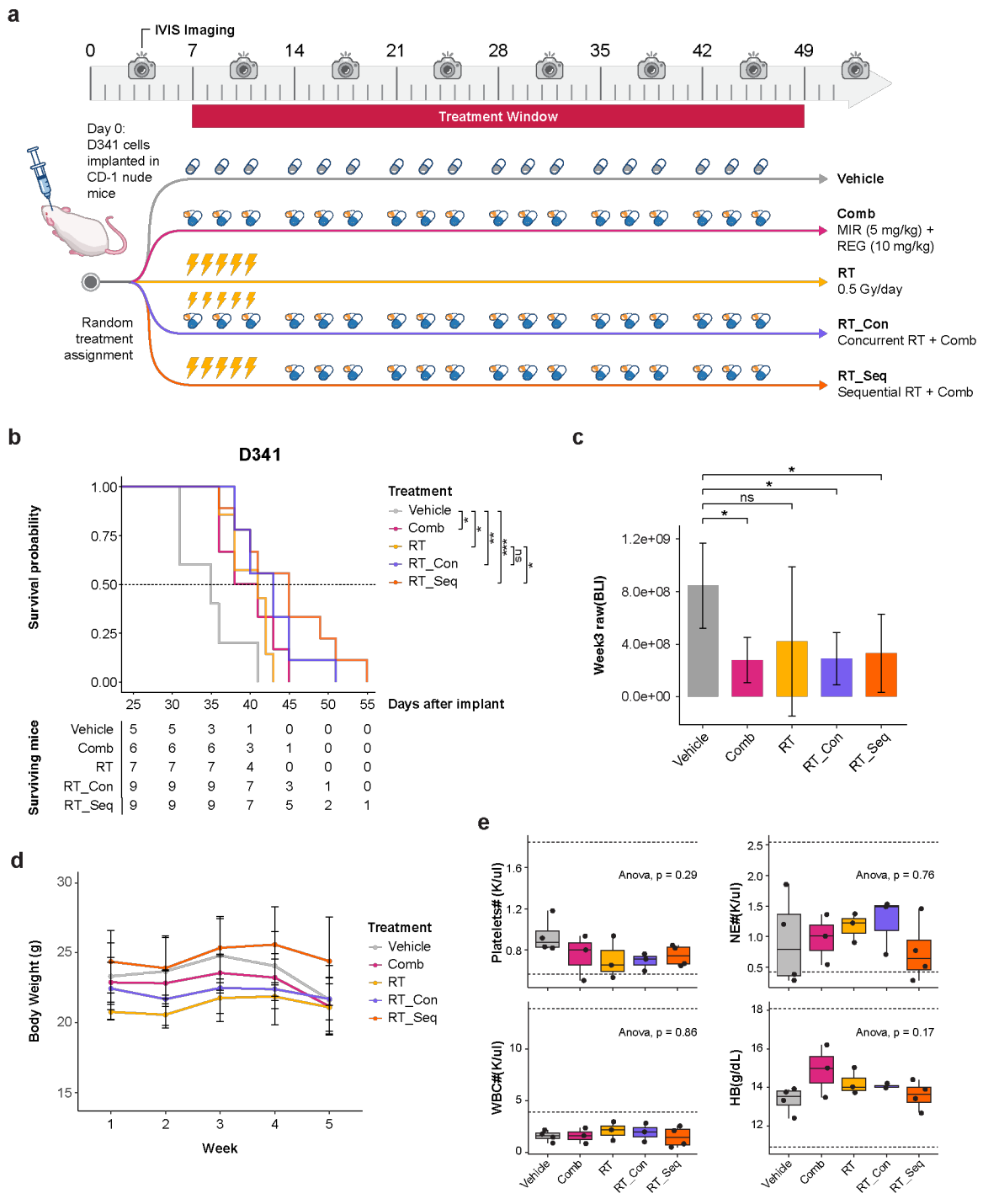

68

69 **Figure S6. Evaluating the combination of mirdametinib, regorafenib, and radiation therapy in the**

70 **D341 Model. a** Schematic of experimental design for drug administration and bioluminescence imaging

(IVIS) in CD-1 nude mice (created with BioRender.com). Mice with intracranial D341 cell implants were randomized into four treatment groups: vehicle (p.o.), drug combination (Comb: mirdametinib at 5 mg/kg p.o. and Regorafenib at 10 mg/kg p.o.), radiation therapy (RT: 0.5 Gy/day for 5 consecutive days), concurrent RT + drug combination (RT_Con), or sequential RT + drug combination (RT_Seq). Treatments commenced one week post-implantation and continued for six weeks. **b** Kaplan–Meier survival curves for mice treated as described in (**a**). Group sizes (n) are indicated in the risk table; log-rank test results: *P < 0.05, **P < 0.01, ***P < 0.001. **c** Quantified bioluminescence imaging (BLI) measurements for each treatment group in the D341 model at week 3 post-treatment enrollment. Data are represented as mean ± SEM. Unpaired two-sided t tests were used. *P < 0.05, ns, not significant. **d** Weekly body weight changes in D341-bearing mice after surgery. Data are represented as mean ± SEM. **e** Endpoint toxicity assessment by complete blood counts (n = 2–4 per group) in the D341 study as shown in (**a**).

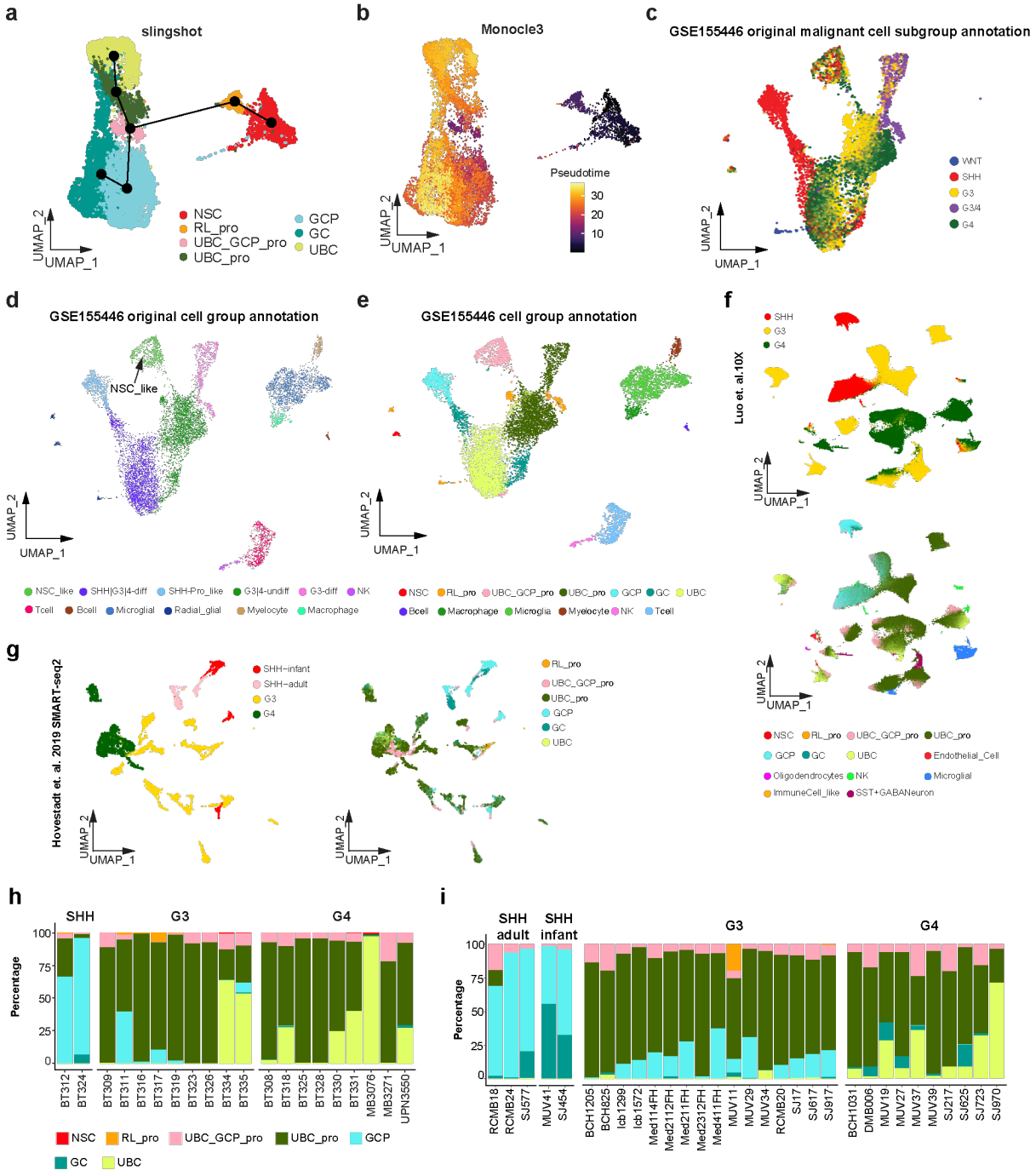

83

84 **Figure S7. Enrichment of UBC_GCP_pro and UBC_pro like tumor cells in G3 and G4 MB revealed**

85 **by scRNA-seq. a** UMAP plot showing developmental trajectories of normal glutamatergic lineage neurons

inferred by Slingshot. **b** UMAP plot of pseudotime trajectories generated by Monocle3, with cells colored by inferred developmental time. **c-d** UMAP plots displaying medulloblastoma tumor subgroup and cell type annotations from the original study (GSE156053; Riemondy et al.). **e** UMAP plot of tumor cell state and normal cell types (GSE156053). **f-g** UMAP plots of two medulloblastoma patient scRNA-seq datasets, annotated by MB subgroup or cell type. **h-i** Proportional distribution of tumor cell states in individual medulloblastoma patients.

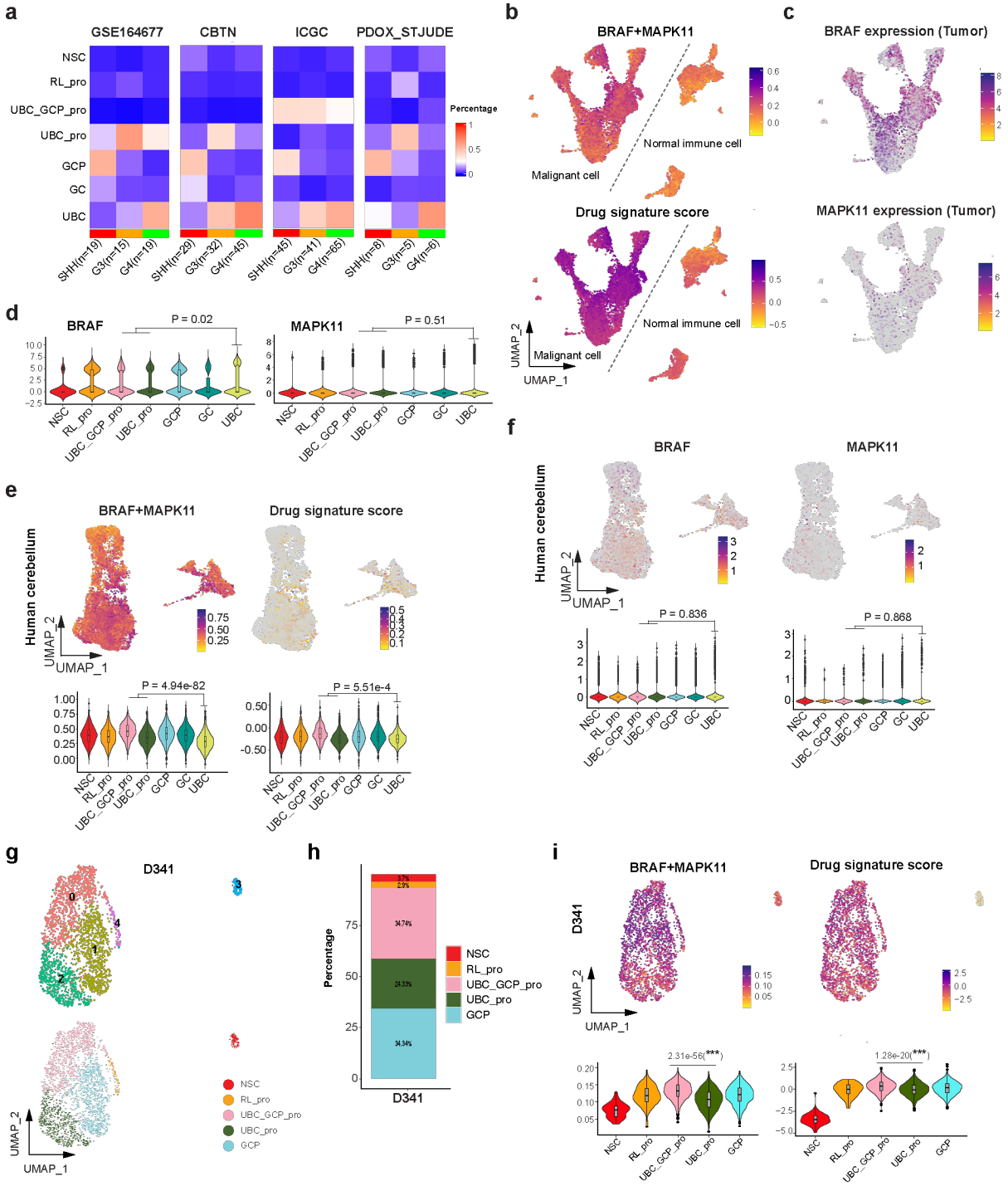

93

94 **Figure S8. UBC_GCP_Pro like tumor cells exhibiting the highest driver activities and drug signature**

95 **scores. a** Transcriptomic deconvolution of RNA-seq profiles via the ReDeconv algorithm across three

independent medulloblastoma patient cohorts and a PDOX dataset, stratified by cellular subpopulations as delineated in Figure 5A. **b** Feature plot of driver combination activities and drug signature scores in malignant cells and normal immune cells (GSE156053). **c-d** Feature and violin plots of BRAF and MAPK11 expression in tumor cells (GSE156053). **e** Feature and violin plots of driver combination activity and drug signature scores in the normal reference. **f** Feature and violin plots of BRAF and MAPK11 expression in the normal reference. **g** UMAP of D341 cell clusters and tumor cell states. **h** Proportional distribution of tumor cell states in D341. **i** Feature and violin plots showing driver combination activities and predicted drug sensitivity scores across tumor cell sate. For (**d**), (**e**), and (**f**), unpaired two-sided t tests were used to compare progenitor-like UBC_GCP_pro and GCP_pro cells with mature-like UBC cells. For (**i**), unpaired two-sided t tests were used to compare UBC_GCP_pro with UBC_pro cells.

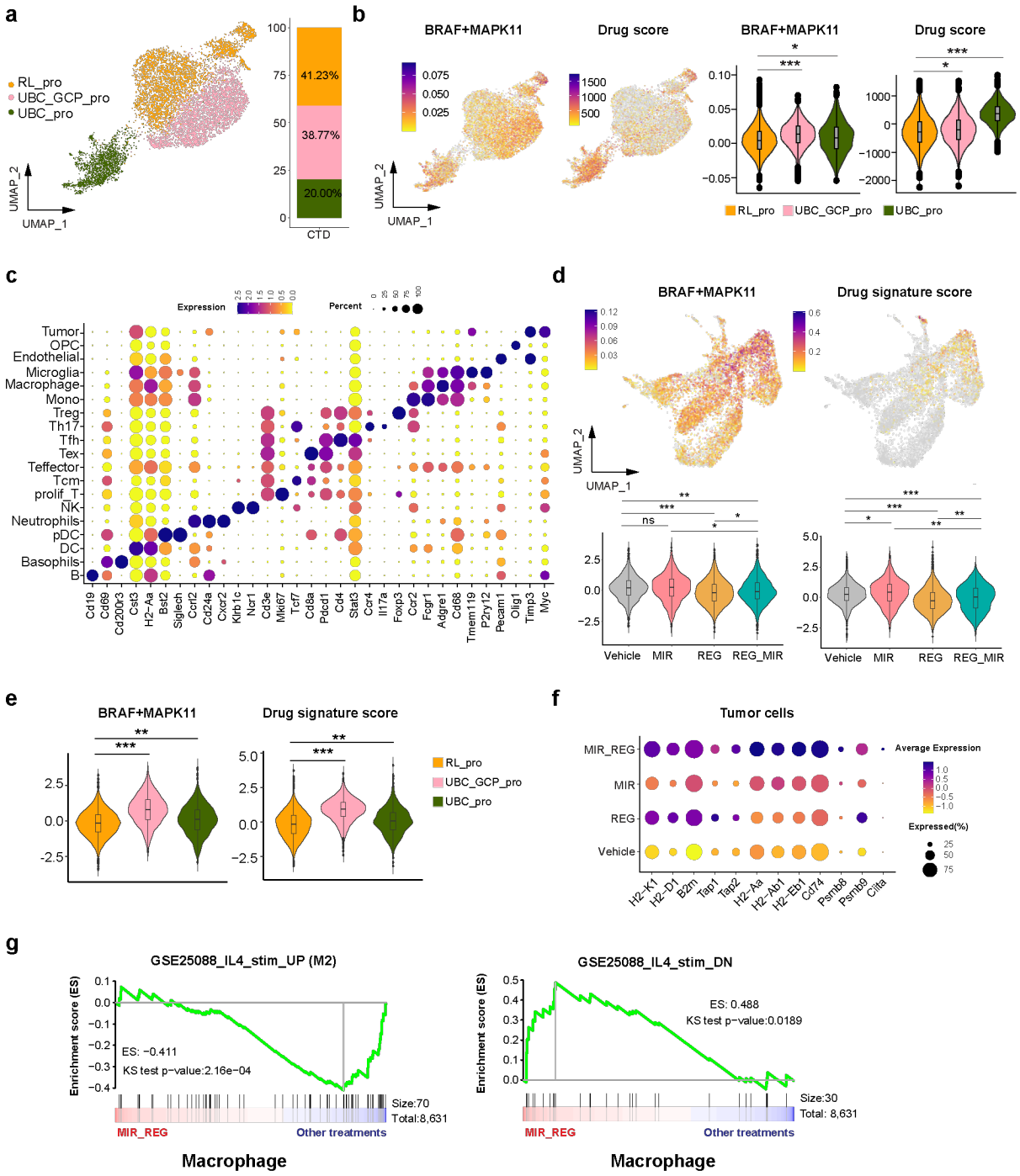

108

109 **Figure S9. Effects of combination therapy on CTD tumor cells and tumor microenvironment. a** Tumor

110 cell states in CTD mapped using normal reference marker genes (Figure 5a), with bar plot showing

proportions of CTD cell states. **b** Feature and violin plots of driver combination activities and predicted drug sensitivity scores across tumor cell states in the CTD model. Two-sided t tests were used to compare RL_pro with UBC_GCP_pro and UBC_pro. *P < 0.05, **P < 1.0e-10, ***P < 1.0e-20. **c** Dot plot showing marker gene expression patterns in immune cell types and tumor cells. **d** Feature and violin plots of driver combination activities and predicted drug sensitivity scores across treatment arms from CTD preclinical study. **e** Violin plots of driver combination activities and predicted drug sensitivity scores across tumor cell states. **f** Dot plot showing antigen presentation gene expression in tumor cells across the four treatment groups. **g** Gene set enrichment analysis of M2-macrophage related genes in macrophages, comparing combination treatment versus other treatment groups.

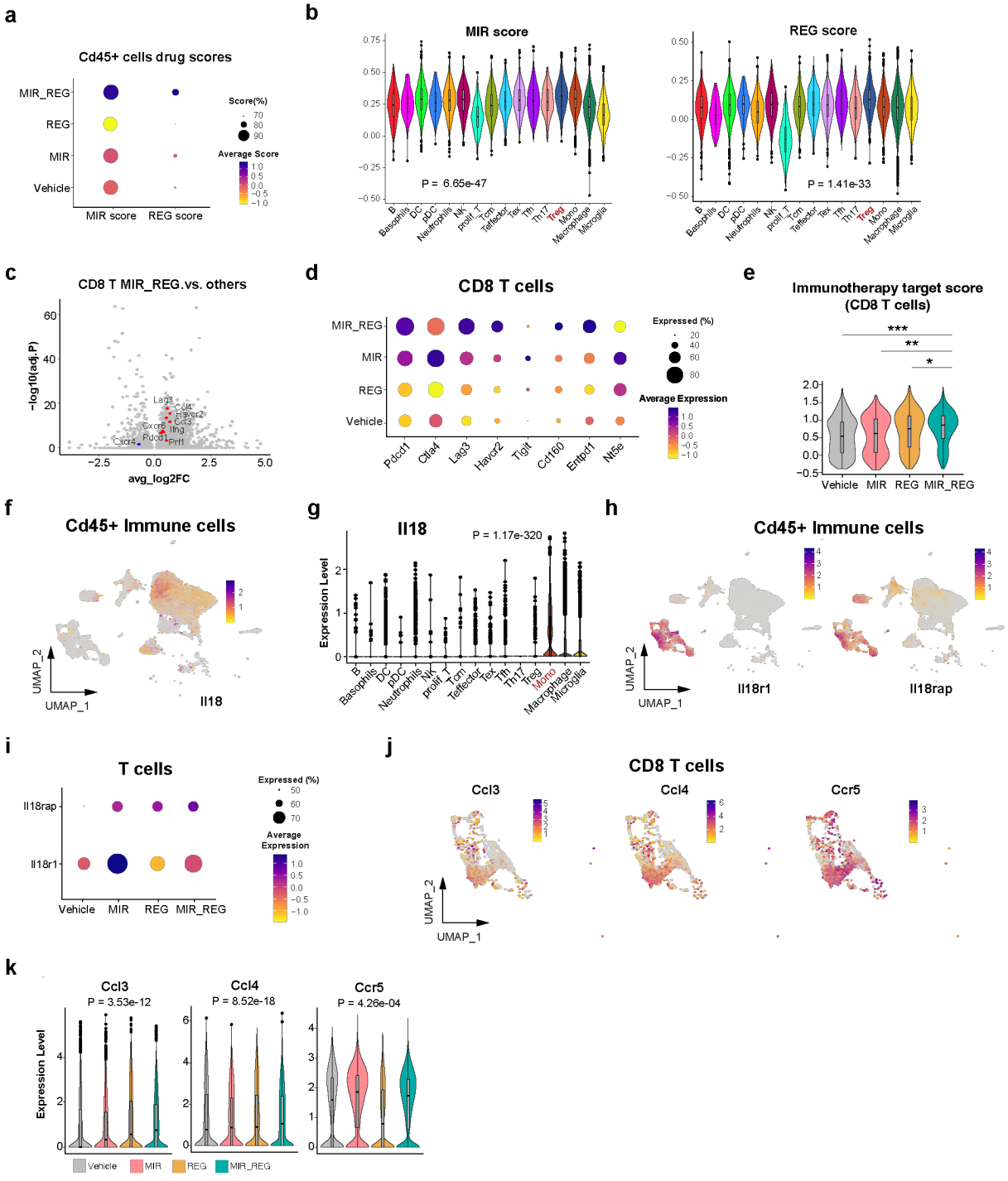

121

122 **Figure S10. The combination of MEK inhibition and regorafenib reconfigures the tumor**

123 **microenvironment. a** Dot plot of mirdametinib and regorafenib drug signature scores in immune cells

across four treatment groups. **b** Violin plot of mirdametinib and regorafenib drug signature scores across immune cell types; two-sided t test comparing Treg cells with other immune cells. **c** Volcano plot of differentially expressed genes in CD8+ T cells from the MIR_REG combination group versus other treatments. **d** Dot plot showing immune therapy–related target gene expression in CD8+ T cells across treatment groups. **e** Module scores for immune therapy target genes; two-sided t tests comparing combination treatment with other groups. *P < 0.05, **P < 1.0e-10, ***P < 1.0e-20. **f** Feature plot of Il18 expression in immune cells from the CTD model. **g** Violin plot of Il18 expression across immune cell types; two-sided t test comparing monocytes with other immune cells. **h** Feature plots of Il18r1 and Il18rap expression in immune cells from the CTD model. **i** Dot plot of Il18r1 and Il18rap expression in T cells across four treatment groups. **j-k** Feature and violin plots of Ccl3, Ccl4, and Ccr5 expression in CD8+ T cells across treatment groups; two-sided t test comparing combination treatment with other groups.

Supplementary Tables

Table S1. Unique genes, drugs, interactions, and drug phases in the six built-in drug-gene interaction databases, related to Figure 1.

Table S2. Bulk RNA-seq profiles from medulloblastoma patient cohorts, related to Figure 1, Supplementary Figure 1 and 8.

Table S3. The correlation between seed-driver activity or expression with MB patient survival, related to Supplementary Figure 1.

Table S4. Seed drug and partner drug libraries for HTS, related to Figure 1 and Supplementary Figure 2.

Table S5. Two-dose combination screening, related to Figure 1 and Supplementary Figure 2.

Table S6. 10-dose combination screening, related to Figure 1.

Table S7. Normal glutamatergic lineage neuron developmental reference 10x scRNA-seq data QC, related to Figure 5.

Table S8. MB patients sample information from the public single-cell RNA-seq datasets, related to Figure 5, Supplementary Figure 7, and 8.

Table S9. GSE155446 MB patient 10x scRNA-seq data QC, related to Figure 5, Supplementary Figure 7 and 8.

Table S10. Hovestadt et al. MB patient SMART-seq2 data QC, related to Supplementary Figure 7.

Table S11. Luo et al. MB patient 10x scRNA-seq data QC, related to Supplementary Figure 7.

Table S12. D341 *in vivo* 10x scRNA-seq data QC table, related to Figure 5.

Table S13. CTD *in vivo* 10x scRNA-seq data QC table, related to Figure 7, Supplementary Figure 9 and 10.

Table S14. M1/G2 microphage signature gene sets, related to Supplementary Figure 9.

Table S15. Trametinib, regorafenib and mirdametinib drug signature genes sets, related to Figure 2, 4, 5 and Supplementary Figure 4, 8, 9 and 10.